Thermal Decomposition of Epoxy Resin Under SF6 Atmosphere

Ren Yang[1], Hongyu Yang[2], Yuhan Wu[2], Dezhi Lin[2], Jun Xue[3], Xiao Zhang[2], Weiqiang Zhang[2,*]

[1]State Grid Shaanxi Electric Power Research Institute, Xi'an 710054, China
[2]Xi'an Key Laboratory of Organometallic Material Chemistry, School of Chemistry and Chemical Engineering, Shaanxi Normal University, Xi'an 710119, China
[3]State Grid Shaanxi Electric Power Company, Xi'an 710054, China

Abstract. The latent fault diagnosis of GIS equipment relies on the electrothermal corrosion information of the decomposition products of SF_6. The thermal decomposition of epoxy resin under atmosphere (SF_6-Epoxy) is essential to reveal the relationship between carbon-based characteristic decomposition components and the degradation of insulating materials. The thermal decomposition process of SF_6-Epoxy was measured using synchronous thermogravimetry(TG)/differential scanning calorimetry(DSC), which unveiled the three pyrolysis stages of temperature range and heat release. The online gas chromatography identified nine decomposition components containing carbon, sulfur and oxygen elements. According to the panoramic pyrolysis reaction mechanism of the SF_6-epoxy system, CO_2, CH_4, SOF_2, H_2S and H_2 were proposed as the characteristic decomposition components for the thermal deterioration of SF_6-Epoxy insulating system.

1. Introduction

With the continuous improvement of the capacity level of the national grid, GIS circuit breakers because of their prominent advantages, such as small footprint, safe and reliable operation, and long access cycles, are widely used in the field of high-voltage and ultrahigh voltage power delivery, which ensures the safe deployment and precise control of power delivery [1]. During long-term charged operation, sulfur hexafluoride (SF_6) and solid insulation materials (epoxy resin epoxy, polytetrafluoroethylene PTFE) within GIS circuit breakers undergo electrothermal decomposition, which leads to overall degradation of the circuit breaker and forms a latent failure hazard [2-4]. The detection of SF_6 oxygen and sulfur decomposition products SO_2, SOF_2 and H_2S can initially diagnose the latent faults of GIS circuit breakers [5-6]. Abnormal working conditions such as arc, abnormal discharge and local overheating in the circuit breaker cause the decomposition of organic solid insulating materials, forming a large number of carbon-based characteristic decomposition products CO, CO_2, CS_2, COS, CH_4, CF_4 [7]. Considering the element balance, the formation of these carbon-based decomposition products must be related to the degradation of organic solid insulating materials in the circuit breaker. However, the information on the degradation elements of the insulating materials contained in these carbon-based decomposition products has not been effectively used, which limits the engineering application of the characteristic decomposition product analysis method in the detection of latent faults. Deeply mining of the electrothermal corrosion information of insulating materials carried by carbon-based decomposition products has important scientific significance and engineering practical value for online monitoring and fault diagnosis of GIS equipment.

Epoxy resins are a class of commonly used organic insulating materials, which are widely used in the production and manufacture of GIS high-voltage electrical equipment such as pot insulators, solid insulating switch cabinets, side sleeve of insulated exchange valve [8]. When these devices suffer from local overheating failure, the epoxy type of materials undergo thermal deterioration. Studying the thermal decomposition reaction of sulfur hexafluoride and epoxy resin system (SF_6-epoxy) to elucidate the relationship between the decomposition products of SF_6 and the degradation of insulating materials is a fundamental way to solve the contradiction between the unitary nature of characteristic components and the diversity of sources. At present, SF_6 epoxy thermal decomposition reaction is poorly studied, and many key questions need to be deeply investigated regarding whether SF_6 is directly involved in the thermal decomposition of epoxy [9] or its secondary decomposition reaction is coupled with the thermal decomposition reaction of epoxy, especially the formation mechanism of carbon-based characteristic decomposition products. *Tang et al.*, first studied the thermal decomposition process of epoxy resin under an atmosphere of SF_6 and detected CF_4, CO_2 and a small amount of CS_2, and proposed CF_4 as a characteristic decomposition product to judge the failure of local overheating on the surface of epoxy resin [10]. While similar pyrolysis experiments only found trace amounts of CF_4 (< 10 ppm) [11]. Considering that arcing, partial discharge, or flash discharge also caused the

* Corresponding author: zwq@snnu.edu

decomposition of SF_6 to produce CF_4, *Zhang et al.*, suggested that CF_4 cannot be used as a judgment for early potential overheating failure. The accurate correspondence between the characteristic decomposition products and the thermal decomposition reaction of insulating materials is the main challenge in judging the latent failure by using the carbon based characteristic decomposition components. In this paper, a synchronous TG / DSC technique was applied to systematically investigate the thermal and mass changes of the thermal decomposition process of SF_6 epoxy. The gas-solid decomposition product composition of the thermal decomposition of bisphenol A-type epoxy resin under an atmosphere of SF_6 was comprehensively analyzed by combining on-line gas chromatography and ambient SEM. The system aligned the thermal decomposition panoramic reaction course of SF_6 epoxy at each weight-loss stage to escape gas and combed out the characteristic decomposition product generation rules, which would be useful for monitoring thermal corrosion of epoxy insulation and provided the experimental basis for diagnosis of GIS latent fault.

2. Result and Discussion

The thermal decomposition of any epoxy resin material starts from the dehydration of the secondary hydroxyl groups on the polymer chain, and then undergo a series of carbon-oxygen bonds, carbon-nitrogen bonds, and carbon-carbon bonds to break, and finally form outgassing products [12]. The entire thermal decomposition process of epoxy resin involves the coupling of multiple chemical transformations, which is a typical complex non-equilibrium multiphase thermodynamic system. In the atmosphere of nitrogen, the pyrolysis of epoxy resin mainly occurs in the range of 400°C, showing a single weight loss; in the air, the oxidation of oxygen accelerates the decomposition of epoxy resin. The main pyrolysis stage of weight loss is advanced to the range of 350°C. The pyrolysis of epoxy resin further coupled with heterogeneous oxidation and decomposition, resulting in a secondary weight loss stage at 521°C [13]. In order to clarify the thermal decomposition reaction process of the SF_6-Epoxy system, We firstly uses the temperature-programming technique to investigate the coupling relationship between the SF_6-Epoxy thermal decomposition heating rate, holding time and the reaction of each decomposition stage, and accurately measures the activation energy of the relevant characteristic decomposition reaction.

2.1 The thermal decomposition process of SF6 - Epoxy system

Fig. 1 presents the synchronous thermal weight loss differential scanning calorimetry (TG-DSC) curves of the SF6 epoxy thermal decomposition process. TG experiment results showed that the first stage dehydration process occurred in the range of 258-342℃ for epoxy resin under SF6 atmosphere, with a weight loss of 18%. The second stage thermal decomposition occurred in the range of 342-481 ℃ with a weight loss of 11%. The final decomposition occurred in the range of 481-629℃, with a weight loss of 46%. Compared to the main thermal weight loss range (around 400 ℃) of N2 epoxy resin,[14] SF6 accelerated the thermal decomposition process of epoxy materials obviously. The decomposition temperature range of SF6 increased by nearly 150 ℃, which indicated that SF6 molecules have chemical corrosion effect on polymer chains. The synchronous DSC curves show that the corresponding characteristic decomposition peak temperatures of these three decomposition stages are 296 ℃, 408 ℃, and 551 ℃. By integrating DSC curve heat flow area, we evaluated the heat release in the primary decomposition stage Δ H = 0.911 kJ / g, the heat release in the secondary decomposition stage Δ H = 0.598 kJ / g, and the ultimate decomposition exotherm Δ H = 9.963 kJ / g.

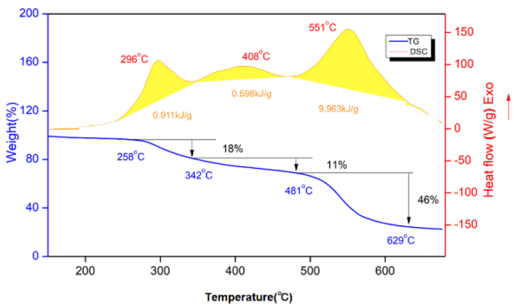

Fig. 1 TG-DSC of thermal decomposition of SF_6-Epoxy (heating rate 20 ℃/min)

The activation energies of the related decomposition processes are calculated from the sample thermal weight loss changes under different heating rates [15]. Table 1 lists the SF_6 epoxy system thermal decomposition parameters under five heating rates with a heating rate of 5-25 ℃ · min^{-1}. The modification of the heating rate did not change the coupling relationship of the three decomposition stages, and increasing the heating rate only accelerated the total weight loss process of the samples.The Kissinger and Flynn wall ozwa methods are commonly used methods to calculate the activation energies for thermal decomposition of polymers [15]. The ramp rates of 15, 20, and 25 ℃/ min and the peak temperatures corresponding to the DTG curves were chosen to calculate apparent activation energy of primary decomposition (E_p) and final decomposition (E_t). By the Kissinger method, E_p was 61.3 kJ/mol and E_t was 256.24 kJ/mol,while E_p was 55.03 kJ/mol and E_t was 255.98 kJ/mol by the Flynn Wall Ozwa method.

Table 1 The influence of heating rate on SF6-Epoxy system

Itemβ/(℃·min^{-1})	5	10	15	20	25
T_i [a](℃)	233	252	249	258	256
T_{exo1} [b] (℃)	267	288	283	296	306
ΔH_1 [c](kJ/g)	1.527	1.317	1.003	0.911	0.780
T_1-T_2 (℃)	233-318	252-340	249-344	258-342	256-362
W_1 [d](%)	23	22	16	18	24
T_{exo2} (℃)	366	376	367	408	398
T_{exo3} (℃)	--	--	411	-	-
ΔH_2(kJ/g)	2.929	0.728	0.695	0.598	0.504
T_2-T_3 (℃)	318-457	340-462	344-462	342-481	362-487
W_2 (%)	29	15	19	11	10
T_{exo4}(℃)	495	511	538	551	556
ΔH_3(kJ/g)	31.49	13.52	11.49	9.963	8.722
T_3-T_4 (℃)	457-535	462-630	462-610	481-629	487-550
W_3 (%)	36	32	33	46	27
W_{end} [e](%)	88	69	68	75	61

[a] The temperature at which weight loss begins; [b] The temperature corresponding to the exothermic peak; [c] The heat flow area of DSC curve to calculate the heat release in the primary decomposition stage; [d] The weight loss; [e] The total weight loss.

It can be concluded that the initial stage of thermal decomposition reaction in SF_6 epoxy system may mainly involve the dehydration process with small apparent activation energy, while the terminal thermal decomposition may involve the formation of C-F with large apparent activation energy of corresponding reaction. The secondary decomposition process involves complex chemical reactions and the whole system mass changes less since the characteristic decomposition peak of DTG curve is not obvious.

2.2 Thermal decomposition products of SF6 - Epoxy system

Reaction force field simulations revealed that the thermal decomposition of epoxy resin mainly produced escaped gas molecules such as CH_2O, H_2O, CO_2, CH_4 and H_2 [16]. In order to comprehensively investigate the thermal decomposition process of the SF_6 epxoy system, three characteristic decomposition stages, the primary pyrolysis stage (below 300℃), the secondary pyrolysis stage (300℃-480℃) as well as the terminal pyrolysis stage (above 480℃) were investigated. We analyzed the products composition of the escaped gas using online gas chromatography. SEM was used to study the morphology and elemental composition of the solid products.

Table 2 lists the three characteristic thermal decomposition stages from 270-517℃ with the escape gas composition generated by the SF_6 epoxy system. During the primary decomposition stage below 300℃, the pyrolysis escape gas products are mainly CO, SO_2 as well as a small amount of hydrogen. This stage of thermal decomposition reaction is mainly the dehydration process of the epoxy resin bulk with that of SF_6. As the pyrolysis temperature increases, the decarbonylation process of the epoxy resin intensifies, with increasing CO concentration. SF_6 epoxy pyrolysis consisted of a series of complex chemical transformation producing a total of nine escape gases CO, CO_2, COS, CH_4, CS_2, SOF_2, SO_2, H_2S and H_2 during the secondary pyrolysis stage at 300-482℃. The secondary reactions involved include, the oxidation of CO by SO_2 to produce COS, which is further hydrolyzed to produce H_2S and CS_2. The water-gas shift of CO and H_2O produce H_2 to CO_2. The epoxy chain contains an active methyl groups in the bipartite position and increasing temperature leads to demethylation. When the temperature increased to 394℃, the concentration of CH_4 increased significantly compared to that at 352℃ or 323 ℃. The concomitant increase in CO, CO_2 and decrease in H_2 concentration within the final pyrolysis stage above 450 ℃, indicating that the dehydration of the epoxy resin complete. The significant decrease of CH_4 content indicated that the demethylation mainly occurred at the secondary thermal decomposition. The decarbonization was through the entire pyrolysis process. The concentration of CO increased, same as the corresponding SOF_2, COS. H_2S is the hydrolysis products of COS. At 517 ℃ for 44 min, H_2 and CH_4 were no longer contained in the pyrolysis gas. The concentrations of CO and CO_2 decreased sharply. When the holding time is extended to 67 min, the concentrations of CO and CO_2 further decrease, indicating that the final pyrolysis is the decarbonylation and decarboxylation.

To further verify the generation pathway of SF_6 epoxy gas products, Fig.4-6 aligned the micromorphologies of the epoxy bulk, secondary pyrolysed solid products with secondary pyrolysed solid products. The elemental contents were listed in Table 3-5. After undergoing ultimate pyrolysis, the epoxy was completely pyrolyzed with no solid product remaining. Microtopographic analysis revealed the irregular bulk solid packing at the micrometer scale for the bulk of the epoxy. Both the primary pyrolyzed solid product and the secondary pyrolyzed solid product showed irregular bulksolid packing were observed. From the above figure, it is

Table 2 Characteristic gaseous products of thermal decomposition of SF6-Epxoy system

		Concentration of Characteristic escaping gaseous product (uL / L)								
	T/℃	CO	CO_2	COS	CS_2	CH_4	H_2	H_2S	SO_2	SOF_2
Primary thermolysis	270	2.30	-	-	-	-	4.20	-	46.06	-
	280	7.43	-	-	-	-	13.63	1.022	66	-
Secondary thermolysis	300	23.84	87.66	0.7215	1.426	3.716	78.3	5.299	62.43	2.616
	305	40.92	85.66	4.232	6.162	12.57	28.8	19	15	2.385
	350	11	25	9.168	2.373	17.88	19.35	57	11	1.563
	451	14.4	38.4	15.53	-	31.99	22.98	20	10	2.744
	482	48.8	80	38.1	9.403	27.76	26.87	20	18	10.46
Final thermolysis	517	2.47	43	56	-	4	74	04	7.5	1.5
	517[a]	18.9	15.02	13.95	-	-	-	15.35	53 8.2	99.44
	517[b]	10.2	98 7.3	8.886	-	-	-	11.75	-	52.95

[a] Heat preservation for 44 min; [b] Heat preservation 67 min.

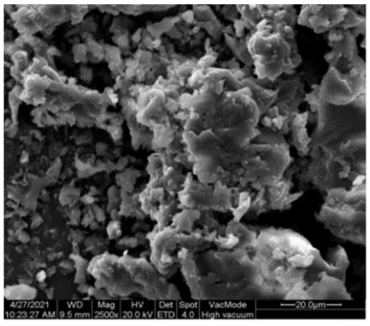

Figure 2 ESEM image of epoxy resin

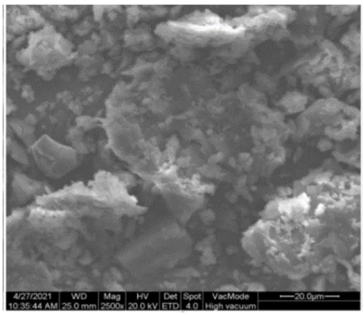

Figure 3 ESEM image of primary pyrolysed solid product

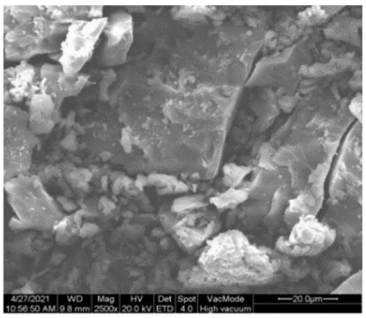

Figure 4 ESEM image of econdary pyrolysed solid product

Table 3 Epoxy element concentration

Epoxy resin		
Element	Wt%	At%
CK	74.15	78.34
OK	15.64	12.41
NK	10.21	9.25

Table 4 Primary pyrolysed solid element concentration

Primary pyrolysed solid product		
Element	Wt%	At%
CK	70.50	75.42
OK	21.63	17.37
NK	7.87	7.22

Table 5 Secondary pyrolysed solid element concentration

Secondary pyrolysed solid product		
Element	Wt%	At%
CK	70.50	75.42
OK	21.63	17.37
NK	7.87	7.22

found that the raw epoxy primary carbonized solid product and the secondary carbonized solid product. These solid decomposition products have less fine agglomerated morphologies relative to the overall morphology of the epoxy resin. The size of the solid becomes larger as the pyrolysis deepening. EDS spectroscopy analysis showed that the elemental composition of the raw epoxy with the solid decomposition products mainly contained carbon, oxygen, and nitrogen, while sulfur and fluorine elements were absent. These results show that during the thermal decomposition process, SF_6 does not directly produce multiphase thermal erosion reaction on epoxy resin. The thermal decomposition of SF_6 epoxy mainly includes the rapid pyrolysis of epoxy resin, and the secondary reaction of SF_6 and gaseous product of epoxy resin. The carbon to oxygen element ratios of the solid samples were 6.3:1, 4.3:1;3.6:1, respectively, indicating that the decarbonylation process of the epoxy resin was significantly faster than the dehydration process, which was consistent with the changes of concentration of gaseous products CO and H_2O related product (H_2S, SOF_2) .

2.3 Summary

According to the synchronous TG/DSC/GC analysis, we propose a panoramic reaction course for thermal decomposition of SF_6-epoxy system (Fig. **5**). The decomposition process starts with the dehydration of epoxy resin. Sequentially, the hydrolysis reaction of SF_6 mutually coupled with the decarbonylation reaction of epoxide. The secondary reactions occur between H_2O, CO, SO_2 which converted to CO_2, COS, CS_2, H_2, and H_2S. These secondary reactions occur mainly in the secondary decomposition stage, in which CO reacts with SO_2 to produce COS, CS_2. From the correspondence consideration of thermal attack of insulating materials, CO is a singular source with SO_2, but its secondary reaction is complicated and not an ideal thermal failure marker characteristic decomposition products. CO_2, although a more complex source, formed as a result of the hydrolysis of CO and COS, with a dramatic increase in its content and a predominant epoxide thermal decarboxylation process at the terminal decomposition stage. Therefore, CO_2 can be used as a characteristic decomposition component for determining the deterioration of epoxy resin hot corrosion at high temperatures (> 500℃). As a singular source characteristic decomposition component, CH_4 can directly correspond to the thermal deterioration of epoxy insulator at 300-500℃. SOF_2, H_2S and H_2 are all produced upon hydrolysis, and a combination of these characteristic components can determine the ultra-low concentration of water of SF_6 epoxy system.

3. Conclusion

In this paper, the material and energy changes of thermal decomposition process of SF_6-Epoxy system were systematically studied, and the temperature range and exothermic heat that characterized the three characteristic pyrolyses were determined. Nine carbon based and sulfoxy decomposition products derived from the pyrolysis of SF_6 epoxy are recognized by on-line GC. After comprehensively analyzing the composition of the decomposition products of gas solids, in this paper, the panoramic reaction course of SF_6 epoxy pyrolysis is resolved, and this information provides an experimental basis for the detection of thermal decomposition failures of epoxy. CO_2 is the characteristic decomposition component in determining the deterioration of the thermal corrosion of epoxy resins at high temperatures (> 500℃), CH4 directly corresponds to the deterioration of the thermal degradation of the epoxy insulation that occurs at 300-500℃, while SOF_2, H_2S, and H_2 are important

evidence to determine the micro water content of SF_6-Epoxy system. Because of the complex secondary reactions, CO and SO_2 are not suitable as thermal failure marker characteristic decomposition components.

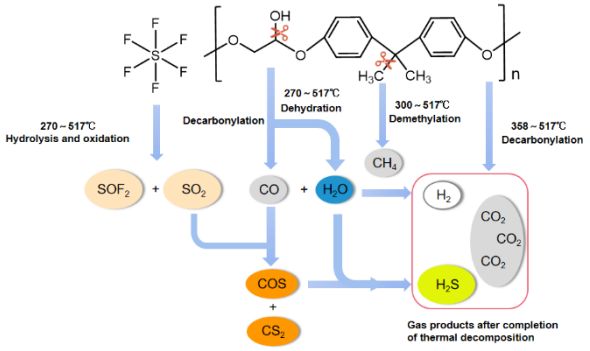

Figure 5. Panoramic analysis of pyrolysis reactions of the SF6 -Epoxy insulating system

Acknowledgements

Project Supported by State Grid Shaanxi Electric Power Company Science and Technology Project (No. 5226ky19004D).

References

1. X. Y. Qin, X. H. Lv, Y. Chen., High Volt. Appar., 57, 72 (2021)
2. X.L. Yan, C.Y.Wang, G. Song, High Volt. Appar., 49, 1 (2013)
3. S. C. Ji, L. P. Zhong, K. Liu, Proc. CSEE, 35, 2318 (2015)
4. J. Tang, D. Yang, F. P. Zeng, Tran. CES, 31, 41 (2016)
5. X. L. Yand, G. Song, C. Y. Wang, Elec. Power Auto. Eq., 34, 83 (2014)
6. Q. Yao, Y. Wang, Y. Liu, High Volt. Appar., 46, 53 (2010)
7. X. L. Yan, Y. S. Ji, C. Y. Wang, Smart Grid, 4, 653 (2016)
8. S. V. Levchik, E. D. Weil, Polymer Intl., 53, 1901 (2010)
9. T. C. Zhao, X. She, Q. Li, High Volt. Appar., 56, 103 (2020)
10. L. Cheng, J. Tang, X. J. Huang, High Volt. Tech., 41, 453 (2015)
11. H. Wen, X. X. Zhang, IEEE Tran. Dielec. Elec. Insl., 26, 1411 (2019)
12. F. Mustata, N. Tudorachi., J. Therm. Anal. Calorim., 125, 97(2016)
13. C. Ma, D. Sánchez-Rodríguez, T.Kamo, J. Hazard. Mater., 412, 125329 (2021)
14. K. Q. Zhou, R. Gao, X. D. Qian, J. Hazard.Mater., 338, 343 (2017)
15. P. Peng, P. Ren, Q. M. Li, High Volt. Tech., 46, 3622 (2020)
16. H. Jin, R. H. Li, X. B. Meng, High Volt. Appar., 54, 44 (2018)
17. H. Wen, X. X. Zhang, R. Xia, Mater., 12, 75 (2019)